

## Diffusion of fluorine ions in yttrium iron garnet

B. Antonini and P. Paroli

*Istituto di Elettronica dello Stato Solido del Consiglio Nazionale delle Ricerche, Via Cineto Romano 42, I-00156 Roma, Italy*

(Received 7 March 1983)

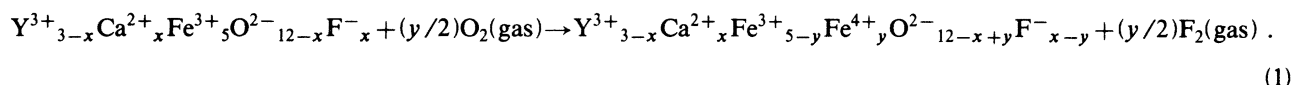
The diffusion of  $F^-$  ions in yttrium iron garnet has been induced for the first time and investigated by magneto-optical techniques. Crystals of composition  $Y_{3-x}Ca_xFe_5O_{12-x}F_x$  (with  $x \approx 0.3$ ) were grown, and diffusion of  $F^-$  ions out of the sample was induced by high-temperature annealing in oxygen. The replacement of  $F^-$  with  $O^{2-}$  ions induces  $Fe^{4+}$  ions, whose magnetic circular dichroism in the near-infrared is used as a sensitive monitor of the diffusion process. This phenomenon can be well described in terms of the classical diffusion equation, with a diffusion coefficient  $D$  uniform and constant, temperature activated according to the law  $D = D_0 \exp(-E/kT)$ , with  $D_0 = 6.5 \pm 1.0 \text{ cm}^2 \text{ s}^{-1}$  and  $E = 3.42 \pm 0.15 \text{ eV}$ . These values might indicate that microscopically the  $F^-$ ,  $O^{2-}$  ion exchange occurs with the intervention of an anion vacancy.

## INTRODUCTION

The technological relevance of magnetic garnets has stimulated a number of studies of both ion substitutions<sup>1</sup> and ion mobility in the garnet structure. Cation exchange between tetrahedral and octahedral sites, useful to control the magnetization of the material, has been reported by Cohen and Chegwidan,<sup>2</sup> and exhaustively investigated by Roschmann in a recent series of papers.<sup>3</sup> Cation exchange within the dodecahedral sublattice has long been assumed<sup>4</sup> to cause the decrease of the growth-induced anisotropy under high-temperature annealings, although no direct evidence of this kind of ion mobility has ever been given. Data by several authors are summarized and discussed in Ref. 3.

As far as the anion mobility is concerned, the self-diffusion of  $O^{2-}$  ions in yttrium iron garnet has been studied by Paladino *et al.*,<sup>5</sup> using radioactive  $^{18}\text{O}$  as a tracer. The diffusion of oxygen vacancies has been observed by Gyorgy *et al.*<sup>6</sup> and quantitatively studied by Metselaar and Larsen<sup>7</sup> in bulk crystals and by LeCraw *et al.*<sup>8</sup> in epitaxial films.

In this paper we report for the first time the diffusion of  $F^-$  ions in yttrium iron garnet (YIG). The technique used consists substantially in starting from a fluorine substituted YIG, of composition  $Y^{3+}_{3-x}Ca^{2+}_xFe^{3+}_5O^{2-}_{12-x}F^-_x$ , and in inducing  $F^-$ -ion migration out of the sample by high-temperature annealing in an oxygen atmosphere. The  $F^-$  ions are replaced by  $O^{2-}$  ions and, to preserve charge neutrality, part of the  $Fe^{3+}$  ions oxidize to  $Fe^{4+}$ , according to the reaction



The  $Fe^{4+}$  ions exhibit relevant optical and magneto-optical activity in the near-infrared optical window of YIG. Therefore, the  $Fe^{4+}$ -ion concentration is used as a convenient and sensitive monitor of the  $F^-$ - $O^{2-}$  interdiffusion phenomenon.

Fluorine substitutions for oxygen could be useful to obtain garnet compositions with low values of the exchange constant, which are required to sustain magnetic bubbles of submicron diameter, as discussed by Ohta *et al.*<sup>9</sup> Also, in principle, fluorine diffusion from the outside to the inside of the material (if technically possible) could be used to form a low magnetization surface layer in bubble films, in order to suppress "hard" bubbles, a procedure conceptually analogous to the gallium diffusion reported by LeCraw *et al.*<sup>10</sup>

## SAMPLES

YIG single crystals were grown by a "flux" technique similar to the one described by Van Uitert *et al.*<sup>11</sup> Calci-

um and fluorine doping was accomplished by adding  $\text{CaF}_2$  to the starting oxides, as done by Ostorero and Makram.<sup>12</sup> The melt composition is shown in Table I. The mixture, in a 100-cm<sup>3</sup> platinum crucible, was heated at a rate of  $40^\circ\text{C h}^{-1}$  to  $1250^\circ\text{C}$ , soaked for 10 h, cooled at  $2^\circ\text{C h}^{-1}$  to  $950^\circ\text{C}$ , and then quenched in air. A few crystals of linear size larger than 1 cm were obtained. The  $\text{CaF}_2$ - $\text{Y}_2\text{O}_3$  mo-

TABLE I. Composition of the flux used to grow the single-crystal samples.

	moles	mol %	grams
PbO	0.250	32.4	55.80
PbF <sub>2</sub>	0.250	32.4	61.3
B <sub>2</sub> O <sub>3</sub>	0.050	6.5	3.48
Fe <sub>2</sub> O <sub>3</sub>	0.154	20.0	24.59
Y <sub>2</sub> O <sub>3</sub>	0.048	6.2	10.84
CaF <sub>2</sub>	0.019	2.5	1.48

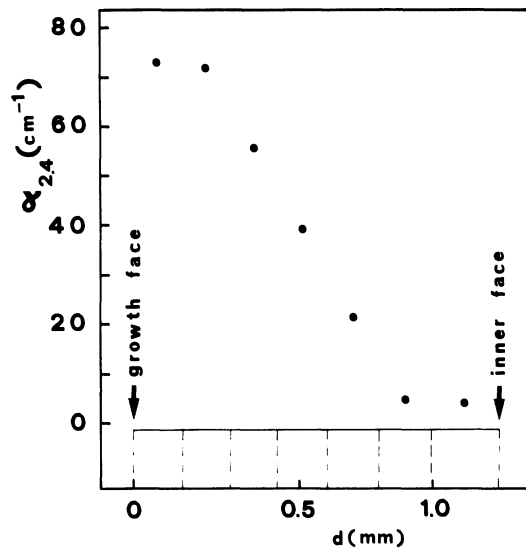


FIG. 1. Optical absorption  $\alpha_{2.4}$  at  $\lambda = 2.4 \mu\text{m}$  as a function of the distance  $d$  from the growth face of the crystal. The crystal slices successively removed to take the data (see text) are indicated in the bottom of the figure with dashed lines.

lar ratio in the starting oxides is such to yield<sup>12</sup> a fluorine content of about 0.2 atom per formula unit in the crystals. This is in reasonable agreement with the  $\text{Fe}^{4+}$ -ion concentration of about 0.3 atom per formula unit (estimated from magnetic circular dichroism and absorption measurements<sup>13</sup>) present in the sample after complete expulsion of fluorine has been obtained, namely when  $y = x$  in Eq. (1).

Several slices were cut parallel to the (110) faces of the largest crystals, mechanically polished with  $0.3\text{-}\mu\text{m}$  alumina powder, and microscopically examined in visible and infrared light. The slices cut closer to the growth faces turned out to be much more absorbent than the ones cut from the inner part of the crystals. To measure this effect, a platelet  $1.1 \text{ mm}$  thick was cut, one of its faces being a (110) growth face. This platelet was thinned by successively removing layers about  $0.15 \text{ mm}$  thick on the side of the growth face, the optical transmission at wavelength  $\lambda = 2.4 \mu\text{m}$  being measured at each step. The average optical absorption  $\alpha_{2.4}$  of each removed layer was obtained by the formula

$$\alpha_{2.4} = -L^{-1} \ln(I'I_0 / I'I'_0),$$

where  $L$  is the layer thickness, and  $I_0, I$  and  $I'_0, I'$  are, respectively, the light intensities incident and transmitted by the slice before and after removing the layer. In Fig. 1  $\alpha_{2.4}$  is plotted versus  $d$ , the distance of the center of the removed layer from the growth surface:  $\alpha_{2.4}$  is seen to approach zero (the expected value<sup>14</sup> for a sample containing only  $\text{Fe}^{3+}$  ions) about  $1 \text{ mm}$  below the growth face.

From the spectral shapes<sup>13</sup> of both optical-absorption and magnetic circular dichroism, the centers optically active in these outer layers of as-grown crystals were unambiguously identified as  $\text{Fe}^{4+}$  ions. It is highly probable that  $\text{Fe}^{4+}$  ions were also responsible for the magnetic anisotropy variation reported in Ref. 12, and ascribed by the

authors to  $\text{Fe}^{2+}$  ions: It is indeed unreasonable to expect the latter to be generated in YIG by doping with a divalent element such as Ca.

In any case, for all measurements reported in the following, platelets of size about  $5 \times 5 \times 0.1 \text{ mm}^3$  were used, cut deeper than  $1 \text{ mm}$  in the crystal, and having  $\alpha_{2.4} < 5 \text{ cm}^{-1}$  in the as-grown state.

## MEASUREMENTS AND DISCUSSION

Each platelet was annealed in 99.95% pure oxygen, at a fixed temperature  $T_a$  ( $1100 \leq T_a \leq 1400^\circ\text{C}$  for different samples), for periods of time ranging from 30 min to several days.

After each annealing step, the total  $\text{Fe}^{4+}$ -ion population was optically measured. Of the two possible optical probes,<sup>13,14</sup> namely absorption and magnetic circular dichroism  $\Delta$ , the latter was chosen, since it provides a more characteristic spectrum and is much less sensitive to small surface defects likely to be produced by high-temperature annealings.  $\Delta$  is defined as

$$\Delta = \alpha_+ - \alpha_- ,$$

where  $\alpha_+$  and  $\alpha_-$  are the absorption coefficients for circularly polarized light when the magnetization of the sample is, respectively, parallel and antiparallel to the spin of the photons. Details on the measuring procedure and apparatus are given in Ref. 15. The spectral range investigated was  $1.2 \leq \lambda \leq 2.4 \mu\text{m}$ , and was reduced on the side of the shorter wavelengths when the samples became too absorbent.

The amplitude  $G(t)$  of the  $\Delta$  spectrum monitors the average concentration of the  $\text{Fe}^{4+}$  centers present in the measured region after an annealing time  $t$ . The correlation of  $G(t)$  with the diffusion phenomenon is as follows.

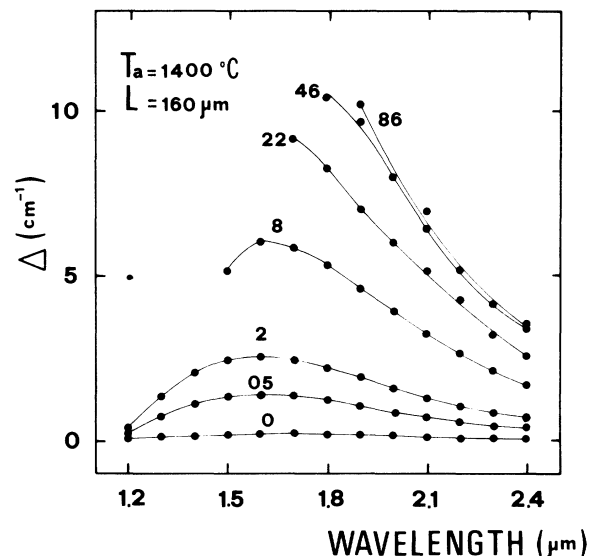


FIG. 2. Magnetic circular dichroism spectra of a sample  $160 \mu\text{m}$  thick, annealed in oxygen at  $T_a = 1400^\circ\text{C}$ . Curves are labeled with the cumulative annealing time expressed in hours. Curve 0 represents the as-grown state.

Consider our sample geometry, namely a platelet normal to the  $z$  axis and of thickness  $L$ . The diffusion of the  $F^-$  ions out of the sample and of the  $O^{2-}$  ions (each with an associated  $Fe^{4+}$  ion) into the sample will take place essentially in the  $z$  direction. Let  $C(t,z)$  be the concentration of the  $Fe^{4+}$  ions present at time  $t$  and height  $z$ , then we have

$$G(t) \propto \frac{1}{L} \int_{-L/2}^{L/2} C(t,z) dz, \quad (2)$$

where  $C(t,z)$  is the solution of the diffusion equation in the  $z$  direction

$$\frac{\partial C(t,z)}{\partial t} = D \frac{\partial^2 C(t,z)}{\partial z^2},$$

and  $D$  is the diffusion coefficient. For our geometry, assuming  $D$  uniform and constant, it is<sup>16</sup>

$$\frac{C(t,z) - C(0,z)}{C(\infty,z) - C(0,z)} = 1 - 4\pi \sum_{k=0}^{\infty} \frac{(-1)^k}{2k+1} \cos\left[(2k+1)\pi \frac{z}{L}\right] \times \exp\left[-(2k+1)^2 \pi^2 \frac{Dt}{L^2}\right]. \quad (3)$$

where  $C(0,z)$  is the concentration (small, and assumed to be uniform) of  $Fe^{4+}$  ions present at  $t \leq 0$ , and  $C(\infty,z)$  is the limiting concentration at  $t \rightarrow \infty$ .

Equations (2) and (3) yield

$$G(t) - G(0) = [G(\infty) - G(0)] \left[ 1 - \sum_{k=0}^{\infty} \frac{8}{(2k+1)^2 \pi^2} \exp\left[-(2k+1)^2 \pi^2 \frac{Dt}{L^2}\right] \right], \quad (4)$$

with the obvious meaning of  $G(0)$  and  $G(\infty)$ . It is important to note that for  $Dt/L^2 < 0.08$ , Eq. (4) can be approximated<sup>7</sup> within 1% by the expression

$$G(t) - G(0) = [G(\infty) - G(0)] 4(Dt/\pi L^2)^{1/2}. \quad (5)$$

An example of dichroism measurements is shown in Fig. 2, where the  $\Delta$  spectra taken after different annealing times at  $T_a = 1400^\circ\text{C}$  are reported. The spectrum labeled 8 (total annealing time 8 h) was arbitrarily chosen as the unit spectrum, in order to measure the relative amplitudes of all the others.

In Fig. 3 the  $\Delta$  spectra of Fig. 2 are plotted versus this unit spectrum. A remarkable linear behavior is found, and the slope of the best fit straight lines are taken as values of  $G(t)$  at  $T_a = 1400^\circ\text{C}$ . This procedure is repeated for all values of  $T_a$ .

Figure 4 shows the time evolution of  $G(t) - G(0)$  at all

the investigated temperatures.  $t^{1/2}$  rather than  $t$  is used as the abscissa, to evidence the linear behavior that, according to Eqs. (4) and (5), is expected to hold for  $0 \leq Dt/L^2 \leq 0.08$ ; that is, for

$$0 \leq \frac{G(t) - G(0)}{G(\infty) - G(0)} \leq 0.63.$$

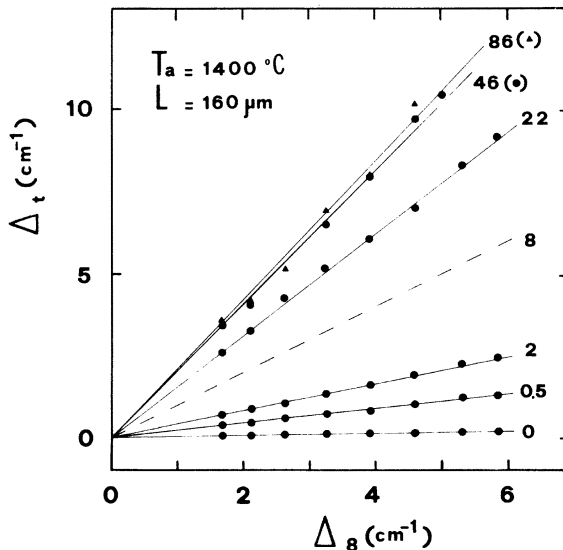


FIG. 3. Magnetic circular dichroism  $\Delta_t$  of the sample of Fig. 2, in the annealing states  $t = 0, 0.5, 2, 22, 46, 86$ , vs  $\Delta_8$  (the dichroism in the state  $t = 8$ ). Continuous straight lines were obtained by least-squares fit.

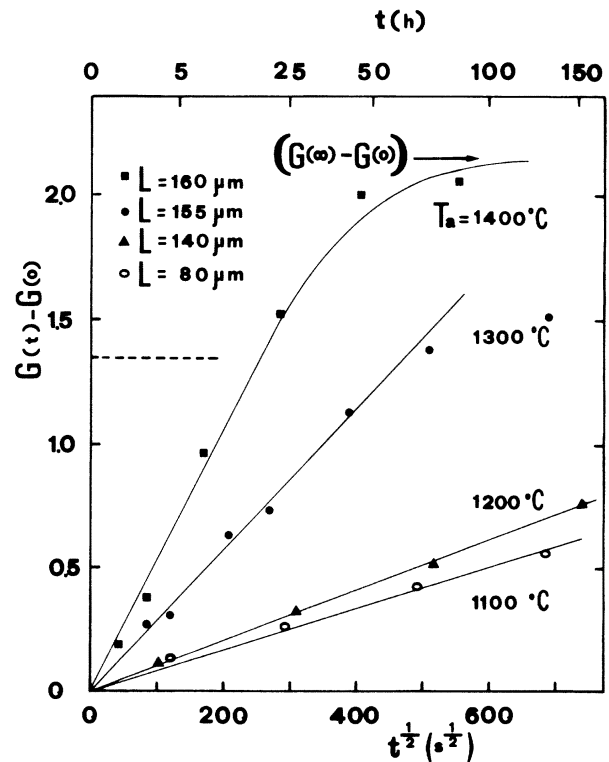


FIG. 4.  $G(t) - G(0)$  (see text) vs the square root of annealing time for various temperatures. Time in hours is reported in the upper scale. The solid line for  $T_a = 1400^\circ\text{C}$  is the least-squares fit with Eq. (4); other solid lines are least-squares fits with Eq. (5). The two equations coincide within 1% for  $G(t) - G(0) \leq 1.35$ , value indicated in the figure by a horizontal dashed line.

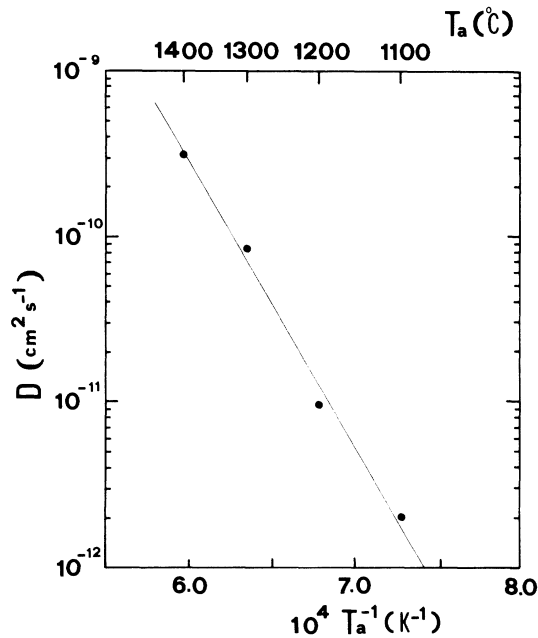


FIG. 5. Fluorine-ion diffusion coefficient  $D$  vs the reciprocal of annealing temperature  $T_a$ . The solid straight line is the least-squares fit with Eq. (6).

Comparison with Fig. 3 of Ref. 7 shows that, at comparable temperature, the  $F^-$ -ion diffusion is much slower than that of oxygen vacancies, as it could be expected.

The diffusion coefficients  $D$  were obtained by fitting the data at  $T_a = 1400^\circ\text{C}$  with Eq. (4), and the data at other temperatures with Eq. (5). In Fig. 5 the logarithm of the  $D$  values thus obtained is plotted versus  $T_a^{-1}$ . A linear behavior is found, so that the temperature dependence of  $D$  can be represented by the equation

$$D = D_0 \exp(-E/kT) \quad (6)$$

with  $D_0 = 6.5 \pm 1.0 \text{ cm}^2 \text{ s}^{-1}$ , and  $E = 3.4 \pm 0.15 \text{ eV}$ . The latter value can be interpreted as the height of the potential barrier to be overcome by  $F^-$  and  $O^{2-}$  ions interdiffusing in the garnet structure.

In principle  $F^-$ - and  $O^{2-}$ -ion exchange can occur either directly (a) or by intervention of an anion vacancy (b). The two cases are schematically shown in Fig. 6, for an idealized two-dimensional triangular lattice. Things are expected to be more complex in the actual garnet structure where six different distances exist between anion sites.<sup>17</sup> Mechanism (a) is expected to involve an activation energy substantially larger than (b), but the probability of the latter should be smaller, being proportional to the product of the relative concentrations of  $F^-$  and anion vacancies. According to Ref. 7, the parameters for the diffusion of oxygen vacancies in YIG are  $D'_0 = 8400 \text{ cm}^2 \text{ s}^{-1}$ , and  $E' = 2.9 \pm 0.1 \text{ eV}$ . The fact that  $E$  differs from  $E'$  by only 20%, while  $D_0 \approx 10^{-3} D'_0$ , might indicate that indeed the  $F^-$ - $O^{2-}$  interdiffusion process has a characteristic energy rather similar to the (anion vacancy)- $O^{2-}$  interdiffusion,

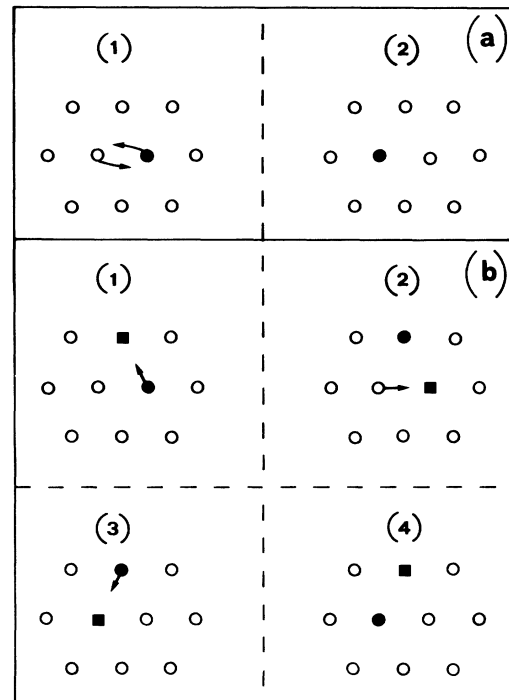


FIG. 6. Schematic mechanism for position exchange between fluorine (●) and oxygen (○) ions: (a) directly, (b) with the intervention of an anion vacancy (■).

but occurs with a much smaller probability. Thus mechanism (b) appears to be dominant over mechanism (a). To further elucidate this point, it would be of interest to study  $F^-$ -ion diffusion in YIG under annealing in partly reducing atmospheres, like mixtures of  $O_2$  and  $N_2$ , as a function of the  $O_2$  partial pressure.

## CONCLUSIONS

The diffusion of  $F^-$  ions in YIG has been induced and studied for the first time. A new measurement technique has been used, consisting in monitoring the magnetic circular dichroism of the  $Fe^{4+}$  centers generated in the garnet by the substitution of  $F^-$  with  $O^{2-}$  ions. This phenomenon can be well described as a classical diffusion process, with a diffusion coefficient  $D$  uniform and constant, independent on diffusing-species concentration.

For  $1100\text{C} \leq T \leq 1400^\circ\text{C}$ ,  $D$  has a temperature dependence of the form  $D = D_0 \exp(-E/kT)$ , with  $D_0 = 6.5 \pm 1.0 \text{ cm}^2 \text{ s}^{-1}$ , and  $E = 3.42 \pm 0.15 \text{ eV}$ . These values might indicate that the dominant elementary microscopic process involved is a site exchange between  $F^-$  and  $O^{2-}$  ions with the intervention of an anion vacancy.

## ACKNOWLEDGMENTS

We thank Professor A. Paoletti and Dr. A. Tucciarone for stimulating discussions, and Mr. L. Tardani for technical assistance.

- <sup>1</sup>S. Geller, *Z. Kristallographie* **125**, 1 (1967).
- <sup>2</sup>H. M. Cohen and R. A. Chegwidden, *J. Appl. Phys.* **37**, 1081 (1966).
- <sup>3</sup>P. Röschmann, *J. Phys. Chem. Solids* **42**, 337 (1981), and references therein.
- <sup>4</sup>A. Rosencwaig, W. J. Tabor, F. B. Hagedorn, and L. G. Van Uitert, *Phys. Rev. Lett.* **26**, 775 (1971); A. Rosencwaig, W. J. Tabor, and R. D. Pierce, *ibid.* **26**, 779 (1971).
- <sup>5</sup>A. E. Paladino, E. A. Maguire, and L. G. Rubin, *J. Am. Ceram. Soc.* **47**, 280 (1964).
- <sup>6</sup>E. M. Gyorgy, J. F. Dillon, and J. P. Remika, *Magnetism and Magnetic Materials—1971 (Chicago)*, Proceedings of the 17th Annual Conference on Magnetism and Magnetic Materials, edited by D. C. Graham and J. J. Rhyne (AIP, New York, 1972), p. 680.
- <sup>7</sup>R. Metselaar and P. K. Larsen, *J. Phys. Chem. Solids* **37**, 599 (1976).
- <sup>8</sup>R. C. LeCraw, E. M. Gyorgy, R. D. Pierce, J. W. Nielsen, S. L. Blank, D. C. Miller, and R. Wolfe, *Appl. Phys. Lett.* **31**, 243 (1977).
- <sup>9</sup>N. Ohta, T. Ikeda, F. Ishida, and Y. Sugita, *IEEE Trans. Mag.* **MAG-16**, 610 (1980).
- <sup>10</sup>R. C. LeCraw, E. M. Gyorgy, and R. Wolfe, *Appl. Phys. Lett.* **24**, 573 (1974).
- <sup>11</sup>L. G. Van Uitert, W. H. Grodkiewicz, and E. F. Dearborn, *J. Am. Ceram. Soc.* **48**, 105 (1965).
- <sup>12</sup>J. Ostorero and H. Makram, *Acad. Sci. Ser. B* **283**, 33 (1976).
- <sup>13</sup>B. Antonini, S. Lagomarsino, A. Paoletti, P. Paroli, R. Tappa, A. Tucciarone, and F. Scarinci, *IEEE Trans. Mag.* **MAG-14**, 877 (1978); B. Antonini, S. L. Blank, S. Lagomarsino, A. Paoletti, P. Paroli, F. Scarinci, and A. Tucciarone, *J. Magn. Mater.* **20**, 216 (1980); B. Antonini, S. L. Blank, S. Lagomarsino, A. Paoletti, P. Paroli, and A. Tucciarone, *IEEE Tran. Mag.* **MAG-17**, 3220 (1981); *J. Appl. Phys.* **53**, 2495 (1982).
- <sup>14</sup>D. L. Wood and J. P. Remeika, *J. Appl. Phys.* **37**, 1232 (1966).
- <sup>15</sup>B. Antonini, A. Paoletti, P. Paroli, A. Tucciarone, J. F. Dillon, E. M. Gyorgy, and J. P. Remeika, *Phys. Rev. B* **12**, 3840 (1975).
- <sup>16</sup>J. Crank, *The Mathematics of Diffusion* (Oxford University Press, Oxford, 1956).
- <sup>17</sup>S. Geller and M. A. Gilleo, *J. Phys. Chem. Solids* **3**, 30 (1957).